

To be submitted to *Astrophys. J.*

Emergence of hyperons in failed supernovae: trigger of the black hole formation

K. Sumiyoshi

Numazu College of Technology, Ooka 3600, Numazu, Shizuoka 410-8501, Japan

sumi@numazu-ct.ac.jp

C. Ishizuka

Department of Cosmosciences, Graduate School of Science, Hokkaido University, Sapporo 060-0810, Japan

chikako@nucl.sci.hokudai.ac.jp

A. Ohnishi

Yukawa Institute for Theoretical Physics, Kyoto University, Kyoto 606-8502, Japan

ohnishi@yukawa.kyoto-u.ac.jp

S. Yamada

Science and Engineering & Advanced Research Institute for Science and Engineering, Waseda University, Okubo, 3-4-1, Shinjuku, Tokyo 169-8555, Japan

shoichi@heap.phys.waseda.ac.jp

and

H. Suzuki

Faculty of Science and Technology, Tokyo University of Science, Yamazaki 2641, Noda, Chiba 278-8510, Japan

suzukih@ph.noda.tus.ac.jp

ABSTRACT

We investigate the emergence of strange baryons in the dynamical collapse of a non-rotating massive star to a black hole by the neutrino-radiation hydrodynamical simulations in general relativity. By following the dynamical formation and collapse of nascent proto-neutron star from the gravitational collapse of a $40M_{\odot}$ star adopting a new hyperonic EOS table, we show that the hyperons do not appear at the core bounce but populate quickly at ~ 0.5 – 0.7 s after the bounce to trigger the re-collapse to a black hole. They start to show up off center owing to high temperatures and later prevail at center when the central density becomes high enough. The neutrino emission from the accreting proto-neutron star with the hyperonic EOS stops much earlier than the corresponding case with a nucleonic EOS while the average energies and luminosities are quite similar between them. These features of neutrino signal are a potential probe of the emergence of new degrees of freedom inside the black hole forming collapse.

Subject headings: supernovae: general — stars: neutron — black hole physics — neutrinos — hydrodynamics — equation of state

1. Introduction

The fate of gravitational collapse of massive stars in the mass range of $\gtrsim 20M_{\odot}$ attracts much attention recently in the attempt to reveal the origin of diversity of supernovae (Nomoto et al. 2007). Their collapse will lead to the formation of black hole and provide us with the test bed for the appearance of exotic particles at high density/temperature.

There appear to be at least two types of massive stellar death in this mass range. Faint supernovae (or failed supernovae) are one of them, having very low explosion energies as observed in SN 1997D and SN 1999br (Nomoto et al. 2007). In contrast to the other branch referred to sometimes as the hypernova branch because of their high explosion energies, their progenitors are supposed to be slowly rotating and collapse to a black hole with no bright optical display. Such a quiet death may consist of a significant fraction ($\sim 30\%$) of all massive stellar collapses and may be detected in the near future, for example, by the planned survey of disappearance of supergiants (Kochanek et al. 2008).

Recent studies by Sumiyoshi et al. (2006, 2007) demonstrated that the neutrino burst from these quiet collapses of massive stars can be used not only as a hallmark of black hole formation but also as a probe of dense matter. In fact, the profile of neutrino burst emitted from the collapsing proto-neutron star born temporarily in the failed explosion has unique characteristics to distinguish them from ordinary supernova neutrinos (See also

Burrows 1988; Liebendoerfer et al. 2004). The duration of neutrino burst is short (~ 1 s) because the neutrino emission is terminated shortly after the black hole formation via the re-collapse of proto-neutron star with intense accretions. The energies and luminosities of neutrinos increase quickly thanks to the rapid contraction of accreting proto-neutron star. These characteristics have been used to search for the black hole formation in the archive of terrestrial neutrino detector (Ikeda et al. 2007) with no positive detection so far.

The future observation of short neutrino bursts, however, would constrain the stiffness of equation of state (EOS) and the appearance of new particles, on which we focus in the current study. The EOS crucially determines when the critical mass is reached by an ever fattening proto-neutron star and, therefore, the duration of neutrino burst. It should be noted that the previous works (Sumiyoshi et al. 2006, 2007) took into account only the nucleonic degree of freedom. If new degrees of freedom such as hyperons (series of strange baryons) appear at some point of the evolution owing to high densities or temperatures, however, then the EOS will become softer (Glendenning 2000), triggering the re-collapse of proto-neutron star earlier, and the neutrino burst may become even shorter.

In this Letter, we report the first serious numerical study of the dynamical collapse of a non-rotating massive star adopting a new EOS with hyperons (Ishizuka et al. 2008). We reveal when the hyperons appear during the stages from the initial collapse of progenitor stars, core bounce and proto-neutron star evolution until the black hole formation. By the neutrino-radiation hydrodynamical simulations, we demonstrate the outcome of hyperon emergence in the dynamics and the neutrino emission. The hyperonic EOS we adopt here is based on the same framework as the nucleonic EOS by Shen et al. (1998a,b). As a natural extension of the former, the latter enables us to extract clearly the effect of hyperons.

We stress that the current scenario of black hole formation is entirely different from the delayed collapse of meta-stable proto-neutron stars and the associated termination of neutrino signals in ~ 1 –100 s (Keil & Janka 1995; Pons et al. 1999; Baumgarte et al. 1996). In fact, the proto-neutron star mass is fixed in successful explosions while it increases continuously and rapidly by the accretion in the failed explosion considered in the current study. The rapid appearance of hyperons in the *dynamical* collapse accompanied by a short neutrino burst is, therefore, clearly different from the characteristics seen in the *quasi-static* cooling of proto-neutron stars (Pons et al. 1999, 2001a,b), in which the emergence of new compositions (hyperons or any other forms) occurs much later when the matter becomes neutron-rich through the deleptonization except for rather extreme choices of interactions. Accordingly, the effect of hyperon mixture on the neutrino signal manifests itself only in the exponential tail of time evolution and hence is hard to detect in observations.

2. Hyperon equation of state

We employ the sets of EOS both with and without the hyperons to explore their influence. As a reference of nucleonic EOS, we adopt the Shen EOS (Shen et al. 1998a,b), which describes the mixture of neutrons, protons, alpha particles and nuclei in the relativistic mean field theory. The hyperonic EOS we adopt here was recently developed by Ishizuka et al. (2008), extending the Shen EOS to SU(3) symmetry to include the octet baryons.¹ It should be stressed that the nucleon sector is not changed from the Shen EOS and, as a result, the low density ($\leq 10^{14}$ g/cm³) part of the hyperonic EOS is connected smoothly with the Shen EOS. The interactions of hyperons are determined by the recent experimental data of hypernuclei. As for the Σ^- -potential in symmetric nuclear matter in particular, we choose the repulsive value (+30 MeV), which is preferred lately. The maximum masses of cold neutron stars by the Shen EOS and the hyperonic EOS are $2.2M_\odot$ and $1.6M_\odot$, respectively. The latter value does not change much even for other choices of interactions and/or the inclusion of thermal pions (Ishizuka et al. 2008). The other sets of the hyperonic EOS, therefore, are expected to give the results not much different from the current ones.

In order to discuss the dependence on the EOS within the nucleonic degree of freedom, we also utilize the profiles of neutrino bursts previously obtained by the Lattimer-Swesty EOS (Lattimer & Swesty 1991) with the incompressibility of 180 MeV, which is softer than the Shen EOS. Its maximum neutron star mass is $1.8M_\odot$. Although other new degrees of freedom such as quarks may appear near the black hole formation, we concentrate here on the hyperon mixture and refer readers to Nakazato et al. (2008), which suggests that the quark mixture may occur only at the last moment of black hole formation. Needless to say, it is important to describe the phase transitions from hyperonic matter to quark matter as well as the meson-condensations consistently (Glendenning 2000). Such a task is being undertaken currently to implement in the numerical simulations.

3. Numerical Simulations

We perform the numerical simulations of neutrino-radiation hydrodynamics in general relativity under the spherical symmetry in the same manner as Sumiyoshi et al. (2006, 2007). We follow the dynamics from the onset of gravitational collapse of a progenitor star, through the core bounce and the post-bounce evolution of compact objects by the accretion of outer layers, up to the formation of the apparent horizon (Nakazato et al. 2006).

¹The tables of the hyperonic EOS are available for public use.

As an initial model, we employ the central part of the progenitor model of a $40M_{\odot}$ star by Woosley & Weaver (1995). We refer to the model using the Shen EOS as model SH and the corresponding model with the Lattimer-Swesty EOS as model LS. We name the new model using the Ishizuka EOS as model IS, which we report mainly in this Letter. For the detailed information on the numerical settings and results of models SH and LS, we refer to Sumiyoshi et al. (2007).

We adopt the conventional weak interaction rates as in the previous numerical simulations (Sumiyoshi et al. 2005). In the current study, we ignore the neutrino-hyperon interactions entirely. This is not so bad an approximation as it seems, however. In fact, owing to the hyper-accretion of outer layers, the neutrino emissions occur dominantly near the surface of the proto-neutron star, where hyperons are scarce. Moreover, since hyperons appear only for ~ 200 ms before the black hole formation, the possible modifications of diffusion rates in the central region, where hyperons are mostly populated, do not have enough time to affect the neutrino fluxes. This reflects the sharp contrast in the durations of neutrino emissions ~ 1 s in the present case and ~ 20 s for the quasi-static proto-neutron star cooling.

4. Numerical results

It is of particular interest to see when hyperons first appear in the collapse of massive stars, since this is the first quantitative investigation utilizing a realistic dynamics and hyperonic EOS. We found that hyperons do not appear at the core bounce, since the central density and temperature are simply not high enough as shown in Fig. 1. In fact, the central density at the core bounce is just above the nuclear matter density. Accordingly, the core bounce and the launch of shock wave followed by the recession, occur exactly in the same way as in model SH. The proto-neutron star without hyperons is born by $t_{pb}=300$ ms, where t_{pb} denotes the time after the bounce.

As the density and temperature increase in the contracting proto-neutron star with the growing mass by the accretion, hyperons first appear off center at $t_{pb} \sim 500$ ms. They soon populate in substantial amount at center and become major compositions by $t_{pb}=680$ ms, at which the central density exceeds three times the nuclear matter density as seen in Fig. 1. This quick appearance of hyperons in the black hole forming collapse is different from what happens in non-accreting proto-neutron stars, where hyperons appear gradually over $\gtrsim 10$ s (Pons et al. 1999) through the cooling and deleptonization. The dynamical collapse to black hole ensues immediately when the proto-neutron star mass reaches its critical value owing to the softening of EOS by the production of hyperons. The black hole is formed at $t_{pb}=682$ ms in model IS, which is much earlier than $t_{pb}=1345$ ms in model SH.

We show two snapshots of the compositions inside the proto-neutron star in Fig. 2. At $t_{pb}=500$ ms (left panel), the mass fraction of hyperons, mostly Λ and Σ^- particles, is a few % at the maximum around 10 km ($0.7M_\odot$ in mass coordinate). The abundance of hyperons becomes significant at $t_{pb}=680$ ms (right panel), since the central density becomes high enough by this time. Λ particles exist as a major composition ($\geq 10\%$) and Ξ^- particles are the next abundant one. Σ^- particles are suppressed at the central region because of the repulsive potential we have chosen. This hierarchy is different from that for attractive potentials, where negatively-charged Σ^- particles are favored (Pons et al. 1999).

It is remarkable that hyperons appear initially off center owing to high temperatures. Although the density at 10 km is not so high at $t_{pb}=500$ ms, the temperature exceeds 50 MeV at the peak (See Fig. 1), where the shock wave is produced and the entropy is generated. The conversion to hyperons occurs through the high energy tail above the hyperon mass of thermal nucleons. This temperature effect keeps the fraction of hyperons around 10 km large even at late stages. The appearance of other particles or phase transitions may also occur owing to the same temperature effect and lead to similar consequences. It is also interesting to note that the hyperon emergence is not controlled by the deleptonization as in the proto-neutron star cooling but driven by the rapid increase of density and temperature in the contracting proto-neutron star. The electron fraction at center remains high (~ 0.3) up to the end whereas it decreases at outer part due to neutronization as seen in Fig. 1.

Whether the emergence of hyperons described above can be probed by the neutrino signal is a matter of great concern. We found that the duration of neutrino burst in model IS is clearly shorter than that in model SH as a result of the earlier black hole formation. We display the time profiles of average energies and luminosities of neutrinos for models IS and SH in Fig. 3. It is apparent that these quantities are quite similar between two models² and only the duration is different. This similarity in neutrino emissions is a direct consequence of the almost identical accretion history irrespective of the presence of hyperons inside the proto-neutron star. In fact, we found that the mass of the proto-neutron star in model IS increases exactly in the same way as in model SH as a function of time. The critical (gravitational) mass, $2.1M_\odot$, is reached earlier in model IS, which is smaller than $2.4M_\odot$ in model SH. We remark here that these critical masses are for the hot proto-neutron stars with neutrinos, being different from those for the cold and neutrino-less neutron stars. It is noticeable that the average energy of $\nu_{\mu/\tau}$ increases faster in model IS than in model SH after $t_{pb}=500$ ms. Because of the hyperon emergence, the contraction of proto-neutron star is accelerated and leads to the quicker temperature increase.

²The slight oscillations in the curves occur owing to insufficient numerical resolutions at the final phase of computations.

The intense and short neutrino burst may be used to infer the properties of the hyperonic matter. Since the hyperon appearance in the proto-neutron star triggers its earlier re-collapse to black hole, we would be able to estimate from the duration of neutrino emissions the critical mass for the conversion to the hyperonic matter. Extra information on the progenitor would be highly helpful (Sumiyoshi et al. 2008) and will be plausible. It should be noted, however, that new degrees of freedom other than hyperons may also result in similar neutrino bursts. The further complication may arise from the uncertainties in the nucleonic EOS. We show the neutrino emissions for model LS in Fig. 3 to elucidate this. The softer LS EOS terminates the neutrino burst at $t_{pb}=566$ ms without hyperons and gives a more rapid rise of the luminosities and energies for all flavors of neutrinos. It is hence necessary to look into more detailed differences of spectra in order to disentangle the degeneracy. The differences in $\nu_{\mu/\tau}$ will be important to distinguish them from one another when neutrino oscillations are taken into account.

5. Summary and Discussions

We demonstrated that the hyperon emergence in the collapse of a non-rotating massive star will produce an intense but short neutrino burst that may be used as a probe into the hyperonic matter. By following the neutrino-radiation hydrodynamics, we revealed that hyperons appear off center at first and prevail also at center just before the black hole formation occurs from the ever accreting proto-neutron star. The resulting neutrino emissions are quite similar to those for the purely nucleonic case and differs only in the earlier termination of neutrino burst. Once hyperons appear during the contraction of proto-neutron star through the mass accretion, they soon trigger the gravitational instability by lowering the critical mass and give rise to even more rapid increases of neutrino energies and luminosities, which are then terminated at the black hole formation.

In order to claim conclusively the appearance of hyperons from observed neutrino signals, further systematic studies must be done. One must discriminate it from other possibilities such as the phase transitions to meson condensations and softer EOSs of nucleonic matter, which may produce similar short neutrino bursts. We remark in passing that the appearance of quarks may not change significantly the duration of neutrino burst (Nakazato et al. 2008) while the density profile of progenitors may affect the behavior of accretion luminosities (Sumiyoshi et al. 2008). The prediction of event rates at neutrino detector facilities with the neutrino oscillations during the propagation being taken into account is currently under way for the models studied so far.

The current numerical results suggest that the appearance of whatever new degrees of

freedom in the black hole forming collapse will be reflected in the energetic neutrino signals that might be detected as a disappearance of massive stars in nearby galaxies in the planned monitoring survey (Kochanek et al. 2008) or in large neutrino facilities (Ando et al. 2005). It will be also interesting to investigate the hyperon emergence in the black hole formations in gamma ray bursts and neutron star mergers.

The numerical simulations were performed at CfCA in NAOJ, JAEA, YITP (Kyoto U.) and RCNP (Osaka U.). This work is partially supported by the Grants-in-Aid for the Scientific Research (18540291, 18540295, 19104006, 19540252) of the MEXT of Japan, Academic Frontier Project of the MEXT, KEK LSSP (07-05) and the 21st-Century COE Program "Holistic Research and Education Center for Physics of Self-organization Systems" in Waseda University.

REFERENCES

Ando, S., Beacom, J. F., & Yuksel, H. 2005, Phys. Rev. Lett., 95, 171101

Baumgarte, T. W., Janka, H.-T., Keil, W., Shapiro, S. L., & Teukolsky, S. A. 1996, Astrophys. J., 468, 823

Burrows, A. 1988, Astrophys. J., 334, 891

Glendenning, N. K. 2000, Compact Stars: Nuclear Physics, Particle Physics, and General Relativity (Springer)

Ikeda, M. et al. 2007, Astrophys. J., 669, 519

Ishizuka, C., Ohnishi, A., Tsubakihara, K., Sumiyoshi, K., & Yamada, S. 2008, J. Phys. G, 35, 085201

Keil, W. & Janka, H.-T. 1995, Astron. Astrophys., 296, 145

Kochanek, C. S. et al. 2008, Astrophys. J., 684, 1336

Lattimer, J. M. & Swesty, F. D. 1991, Nucl. Phys., A535, 331

Liebendoerfer, M. et al. 2004, Astrophys. J. Suppl., 150, 263

Nakazato, K., Sumiyoshi, K., & Yamada, S. 2006, Astrophys. J., 645, 519

—. 2008, Phys. Rev., D77, 103006

Nomoto, K. et al. 2007, in Supernova 1987A: 20 Years After: Supernovae and Gamma-Ray Bursters, arXiv:0707.2187

Pons, J. A., Miralles, J. A., Prakash, M., & Lattimer, J. M. 2001a, *Astrophys. J.*, 553, 382

Pons, J. A., Reddy, S., Prakash, M., Lattimer, J. M., & Miralles, J. A. 1999, *Astrophys. J.*, 513, 780

Pons, J. A., Steiner, A. W., Prakash, M., & Lattimer, J. M. 2001b, *Phys. Rev. Lett.*, 86, 5223

Shen, H., Toki, H., Oyamatsu, K., & Sumiyoshi, K. 1998a, *Nucl. Phys.*, A637, 435

—. 1998b, *Prog. Thoer. Phys.*, 100, 1013

Sumiyoshi, K., Yamada, S., & Suzuki, H. 2007, *Astrophys. J.*, 667, 382

—. 2008, *Astrophys. J.*, 688, in press

Sumiyoshi, K., Yamada, S., Suzuki, H., & Chiba, S. 2006, *Phys. Rev. Lett.*, 97, 091101

Sumiyoshi, K., Yamada, S., Suzuki, H., Shen, H., Chiba, S., & Toki, H. 2005, *Astrophys. J.*, 629, 922

Woosley, S. E. & Weaver, T. 1995, *Astrophys. J. Suppl.*, 101, 181

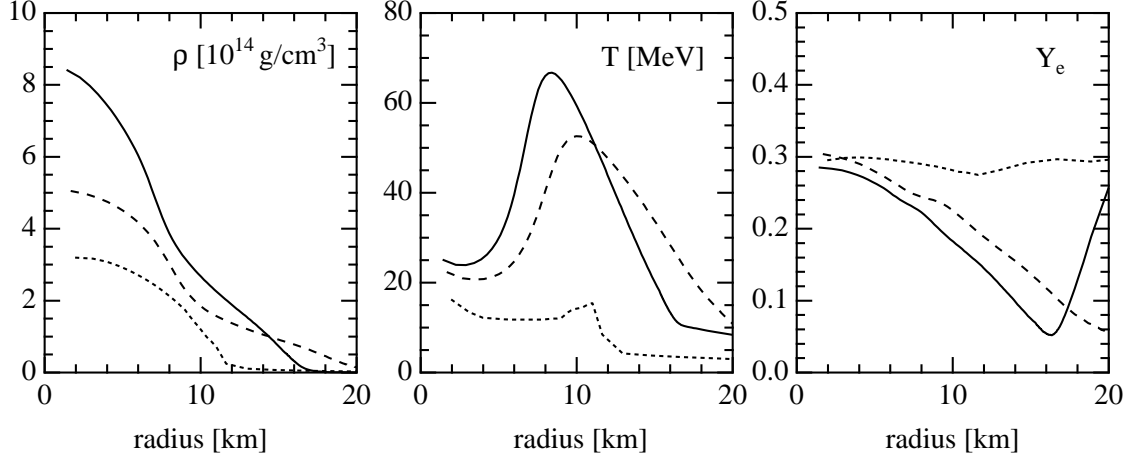


Fig. 1.— Density (left), temperature (center) and electron fraction (right) profiles for IS at $t_{pb}=0$, 500 and 680 ms are shown by dotted, dashed and solid curves, respectively, as a function of radius.

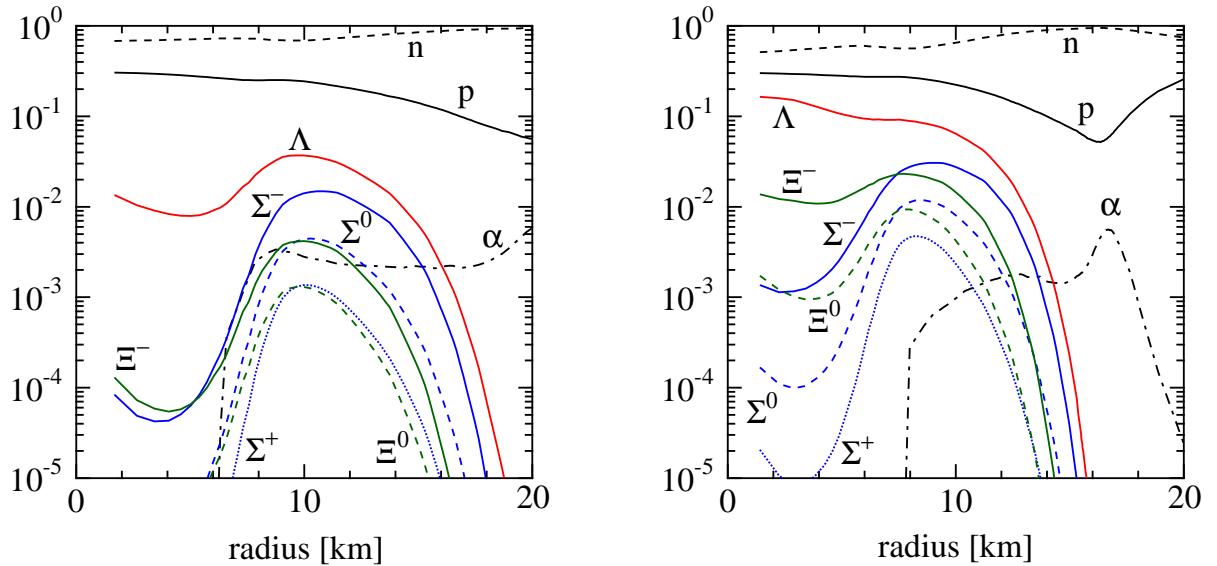


Fig. 2.— Mass fractions of hyperons in model IS are shown as a function of radius at $t_{pb}=500$ (left) and 680 ms (right).

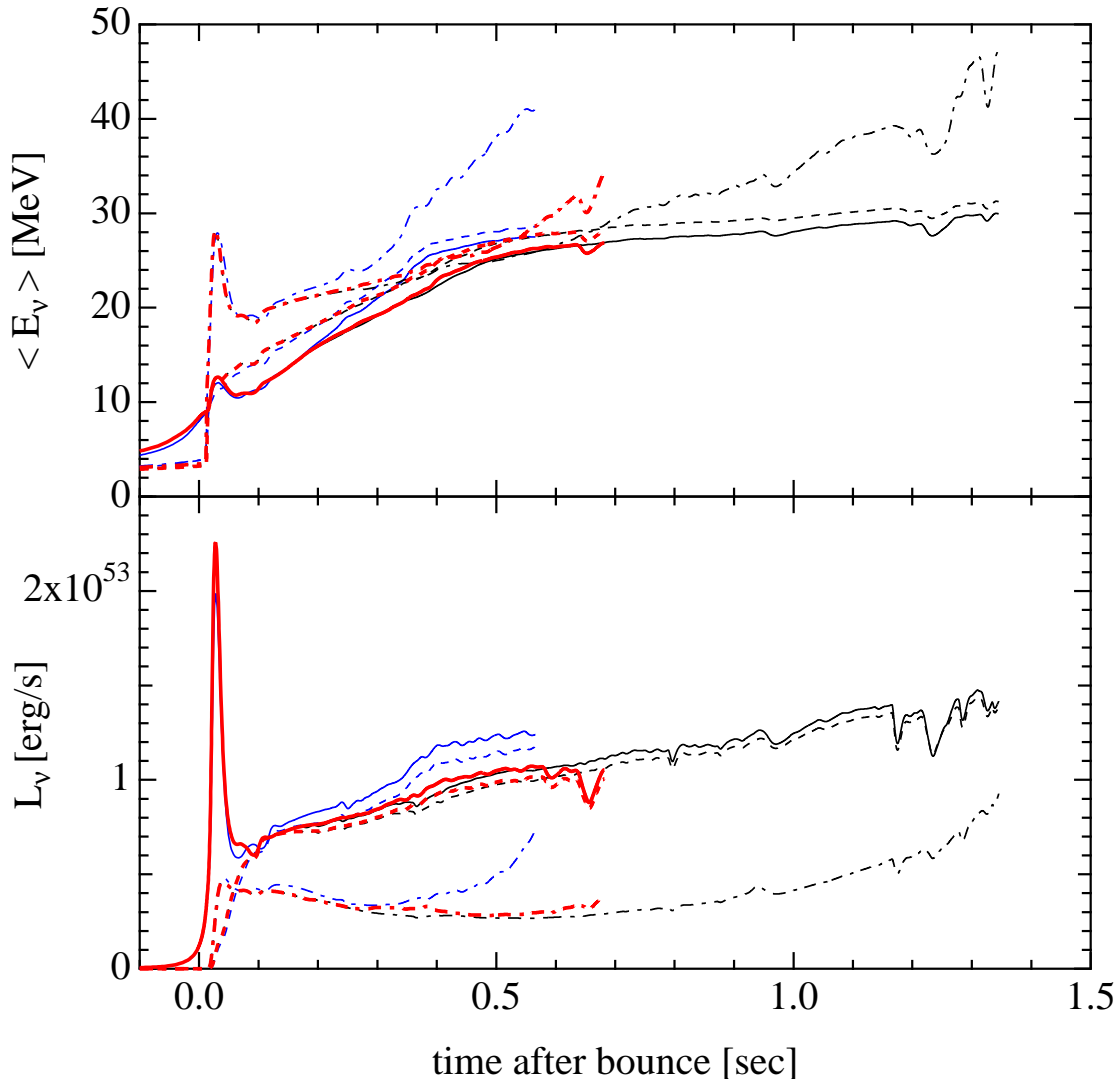


Fig. 3.— Average energies and luminosities of ν_e (solid), $\bar{\nu}_e$ (dashed) and $\nu_{\mu/\tau}$ (dash-dotted) for model IS are shown as a function of time after bounce. The results for model SH and LS are shown by thin lines with the same notation.